Biochemical and Biophysical Research Communications 450 (2014) 1297–1303

Contents lists available at ScienceDirect

Biochemical and Biophysical Research Communications

journal homepage: www.elsevier.com/locate/ybbrc

MicroRNA-203 accelerates apoptosis in LPS-stimulated alveolar epithelial cells by targeting PIK3CA

Xian-Fu Ke [a], Jie Fang [a], Xiao-Ning Wu [b], Chen-Huan Yu [a,*]

[a] Zhejiang Academy of Medical Sciences, Hangzhou 310013, China
[b] Zhejiang Medical College, Hangzhou 310053, China

ARTICLE INFO

Article history:
Received 22 June 2014
Available online 1 July 2014

Keywords:
microRNA-203
PIK3CA
Apoptosis
Lipopolysaccharide

ABSTRACT

The pathogenesis of endotoxin-induced acute lung injury (ALI) remains obscure and has not been well elucidated hitherto. Recently, microRNAs have distinct expression profiles in innate immunity, inflammation, and infection. However, the functions of microRNAs in ALI remain unknown. In this study, the functions of microRNAs in the development of ALI were investigated to identify potential drug targets. MicroRNA-203 (miR-203) expression in the lung tissues of lipopolysaccharide (LPS)-challenged mice was found to be significantly upregulated and peaked 5 d post-LPS injection. MiR-203 overexpression in A549 cells significantly promoted cell apoptosis by inducing S-phase cell-cycle arrest. MiR-203 overexpression also inhibited the protein expression of phosphoinositide 3-kinase catalytic subunit alpha (PIK3CA), a direct target of miR-203 identified by bioinformatics, thereby suppressing the PI3K/Akt pathway. Moreover, repressed miR-203 effectively attenuated LPS-induced interstitial pneumonia. Therefore, regulating or inhibiting miR-203 may be of therapeutic potential in pneumonia and ALI.

1. Introduction

Acute lung injury/acute respiratory distress syndrome (ALI/ARDS) is a progressive syndrome with a high incidence and mortality rate [1]. Infection, particularly induced by Gram-negative bacteria, is an important etiological factor for ALI. It is characterized by the fulminant inflammatory and apoptotic responses that may cause morphological and functional injury to the respiratory membrane [2]. Numerous synthetic or natural chemicals have been widely investigated to reduce the inflammatory and pro-apoptotic responses during the course of sepsis-induced ALI [3–6]. However, the translational application of these results to clinical treatment remains limited. Therefore, further investigation of the molecular mechanism that regulates apoptosis and inflammation is required to provide a novel therapeutic intervention for ALI.

MicroRNAs (miRNAs) comprise a class of 18–23 nucleotide long non-coding RNAs, which have critical functions in post-transcriptional degradation of target mRNA or inhibition of protein synthesis through binding to specific sites of the target mRNA. MiRNAs have important functions in a wide spectrum of biological processes, including proliferation, differentiation, metabolism, apoptosis, and innate immunity [7]. Increasing evidence has shown that miRNAs can function as apoptosis suppressors (e.g., miR-107, miR-20a, and miR-886) [8–10] or enhancers (e.g., miR-29b and miR-193b) [11,12]. Much progress in determining miRNA function on solid tumor has been achieved in the past decades. However, elucidating the occurrence and mechanism of apoptosis during LPS-induced ALI has not been paid much attention.

To define the LPS-induced miRNA pattern, we conducted a miRNA microarray screen that resulted in a set of differentially regulated miRNAs, including miRNA-203 (miR-203), which was deregulated in lung tissues of ALI mice. MiR-203 upregulation significantly inhibited LPS-induced apoptosis, whereas its inhibitor-mediated downregulation attenuated cellular injury. A bioinformatics search revealed that phosphoinositide 3-kinase catalytic subunit alpha (PIK3CA) was one of the targets of miR-203. PIK3CA has an important function in the apoptosis of lung epithelial cells [13]. Thus, we investigated the function of miR-203 in apoptosis in human lung epithelial A549 cells.

2. Materials and methods

2.1. Mice and preparation of ALI model

Male ICR mice (18–22 g) were purchased from the Zhejiang Center of Laboratory Animals. All surgical and care procedures

* Corresponding author. Fax: +86 0571 88215499.
E-mail address: yuchenhuan2002@163.com (C.-H. Yu).

http://dx.doi.org/10.1016/j.bbrc.2014.06.125
0006-291X/

administered to the animals were in accordance with the institutional guidelines of Zhejiang Academy of Medical Sciences. The animals were housed in a specific pathogen-free condition in groups of five per standard cage on 12 h light/dark cycle. The air temperature was maintained at 22 °C ± 2 °C. Ten mice were anesthetized with diethyl ether and then intravenously injected with 0.1 mg of lipopolysaccharide (LPS) in 25 μL of phosphate-buffered solution (PBS) [14]. Another 10 normal mice were used as controls. Lung tissues were harvested in five duplicates every 48 and 120 h post-LPS challenge (pneumonitis at the initial and late stages).

2.2. Microarray analysis

Total RNA was harvested from LPS-infected lung tissues on days 2 and 5 post-infection using TRIzol (Invitrogen) and miRNeasy mini kit (QIAGEN). After passing the RNA quantity measurement using the NanoDrop 1000, the samples were labeled using the miRCURY™ Hy3™/Hy5™ power labeling kit and were hybridized on the miRCURY™ LNA Array (v18.0). The slides were scanned using the Axon GenePix 4000B microarray scanner. The scanned images were then imported into GenePix Pro 6.0 software (Axon) for grid alignment and data extraction. Replicated miRNAs were averaged. MiRNAs with intensities $\geqslant$30 in all samples were chosen to calculate the normalization factor. The expressed data were normalized using the median normalization. Differentially expressed miRNAs were then identified through Fold Change filtering (Fold Change >2.0). Finally, hierarchical clustering was performed to show distinguishable miRNA expression profiling among samples. TargetScan and miRNA.org were used for miRNA target prediction.

2.3. Cell culture

A549 is a human pulmonary epithelial cell line that was cultured in RPMI (1640) medium with 2 mM of glutamine, 10 U/mL of penicillin, 10 μg/mL of streptomycin, and 10% fetal bovine serum at 37 °C in a CO_2 incubator. A549 cell monolayers were inoculated at a 50% tissue culture infective dose of 100/cell. After 1 h of inoculation, the cells were washed twice with PBS and supplemented with maintenance media.

2.4. Real-time PCR

For miR-203 analysis, total RNA was isolated from cells using the MicroRNA Extraction and Purification Kit (Novland, Shanghai, China). Real-time PCR was performed using two-step Stemaim-it miR qRT-PCR Quantitation Kit (SYBR Green) (Novland, shanghai, China) on BIO-RAD IQ5 real-time PCR instrument. Specific primers and probes for mature miR-203 and snRNA RNU6B were obtained from Genepharm, Shanghai, China. All reactions were conducted in triplicate. Quantitative normalization was performed on U6 and β-actin for miRNA and mRNA detection, respectively.

2.5. Luciferase reporter assay

To determine whether PIK3CA is a direct target of miR-203, we cloned the miR-203-predicted target sequence that was contained within its 3′-untranslated region (3′-UTR) downstream of a luciferase gene in the p-miR-reporter luciferase plasmid (Biotech, Shanghai). The lysate was assayed using Dual-Glo luciferase assay system (E1960; Promega, USA) and was measured by a luminometer (EG&G Berthold, Wildbad, Germany).

2.6. Cell apoptosis and cell cycle analysis

The cells were seeded into 96-well plates at 1×10^5 cells/well for the analysis of cell viability. After the treatment, A549 cells were suspended in binding buffer containing annexin V-FITC and propidium iodide (PI) according to manufacturer's instructions (KeyGen) and assessed by flow cytometry. To analyze the cell cycle, cells were prepared using a Cell Cycle Detection Kit (KeyGen) and analyzed with a FACSCan flow cytometer (BD Biosciences, USA).

2.7. Western blot analysis

Total cell protein extracts (20 μg) were separated by 10% SDS polyacrylamide gel electrophoresis and then transferred onto a polyvinylidene difluoride membrane (Millipore, USA). The membrane was blocked for 1 h in PBST with 5% non-fat milk at 4 °C. Then, the blots were incubated with primary antibodies against PIK3CA, Akt, p-Akt, caspase-9, Bad, Bax and β-actin (Santa Cruz, USA) followed by horseradish peroxidase-conjugated secondary antibody and detected by chemiluminescence detection kit (Millipore, Billerico, MA, USA). The intensity of protein fragments was quantified using Image-Pro Plus software.

2.8. Pathological analysis

The LPS-infected mice were divided into two groups. Mice in the model control group received 50 μL of 0.9% saline by the vena caudal. By contrast, mice in the miR-203-treated group were intravenously injected with miR-203 antagomir (40 μg/g) once a day on days 2 and 4 post-infection. The mice were euthanized 5 d post-LPS challenge. The wet weight of whole lung was determined to assess tissue edema as reported previously [14]. The middle lobe of the right lung were harvested and fixed in 10% buffered formalin, embedded in paraffin, sectioned, and stained with hematoxylin and eosin. Cell death was detected by using terminal transferase dUTP nick end labeling (TUNEL). Pathological changes in the lung tissues were observed under a light microscope.

2.9. PIK3CA rescue experiments

The coding sequence of human PIK3CA excluding its 3′-UTR was inserted into the pTarget vector (GeneCopoeia, USA). The A549 cells were co-transfected with negative control oligos or miR-203 mimics and with empty pTarget vector or pTarget-PIK3CA. Forty-eight hours after transfection, the cells were harvested and analyzed using cell cycle assay by flow cytometry, which was described above. Western blotting was also used to signify the expression of PIK3CA.

2.10. Statistical analysis

All parameters were recorded for individuals within all groups. The statistical comparisons of data were implemented using ANOVA and *t*-test in the SPSS 13.0 system. P value < 0.01 was considered significant.

3. Results

3.1. MiRNA expression profiles and qPCR validation in the lung tissues of LPS-challenged mice

The genome-wide miRNA expression profiles of the lung tissues in the normal and model control groups were analyzed on days 2 and 5 post-infection. After normalization, 38 upregulated and 37 downregulated miRNAs were found in the lung tissues of LPS-challenged mice compared with those in the normal control group. Using a Venn diagram, similar patterns on days 2 and 5 post-infection were acquired (Fig. 1). Among these eight significantly changed miRNAs, miR-203 had the remarkable fold change. Moreover,

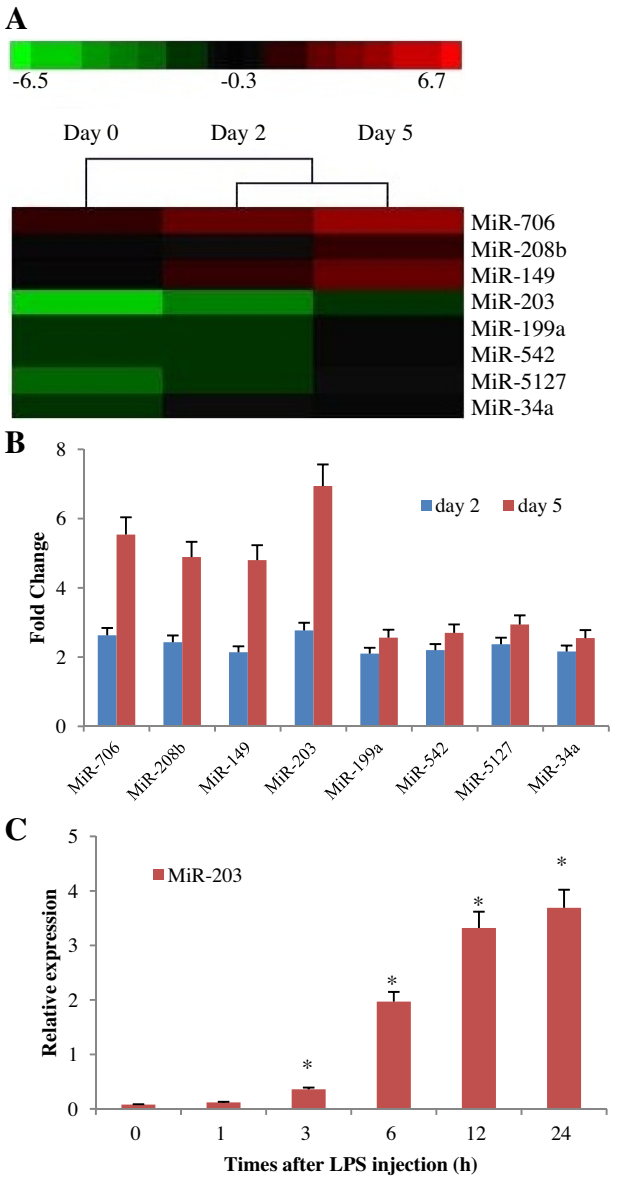

Fig. 1. MiRNA expression in lung tissue of ALI mice. (A) Heat map of microRNA (miRNA) profiles represented the significantly regulated miRNAs. (B) Listing of miRNAs in heat map with fold change. Among those, miR-203 was the highest expressed miRNA in lung tissue of ALI mice compared with mock-infected mice. (C) MiR-203 expression was validated by qPCR in mice challenged with LPS. Bars are represented from three independent experiments. $^{*}P < 0.01$ vs. mock injection.

the upregulation of miR-203 was confirmed by qPCR after LPS challenge in mice (based on ethics, the animals were sacrificed by sodium pentobarbital due to the sudden mass death of mice 6 d post-challenge). MiR-203 expression was substantially upregulated, and the peak value was observed 5 d post-challenge (Fig. 1C).

3.2. PIK3CA as a target of miR-203

We further predicted the target genes of miR-203 using TargetScan and miRNA.org, and identified PIK3CA as a potential target of miR-203. We constructed a firefly luciferase reporter containing the potential binding site for miR-203 in PIK3CA 3′-UTR (Fig. 2A); PIK3CA 3′-UTR plasmid and miR-203 mimic were then co-transfected into A549 cells. The reporter assay showed that miR-203 could significantly inhibit luciferase expression. However, this effect was abolished when two nucleotides in the miR-124 seed binding site

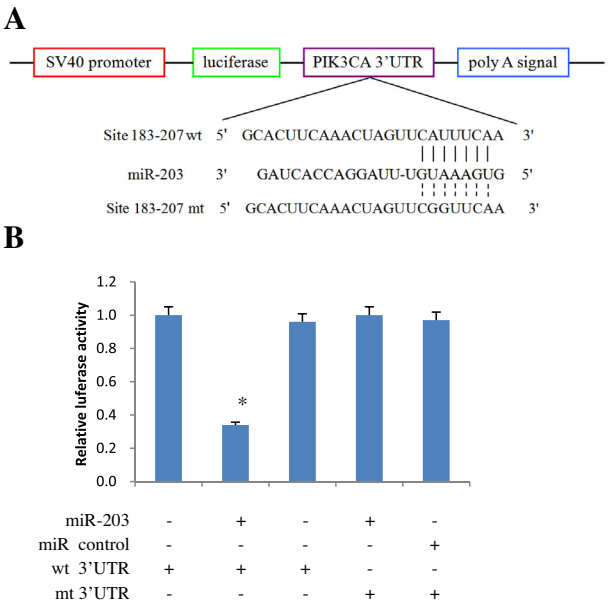

Fig. 2. PIK3CA is a direct target of miR-203. (A) Diagram of PIK3CA 3′-UTR-containing reporter constructs. (B) Relative repression of luciferase expression standardized to a transfection control was analyzed by luciferase reporter assays. MiR report construct, containing a wild-type or a mutated PIK3CA 3′-UTR, were transfected into A549 cells which were infected by miR-control-lentivirus or miR-203-lentivirus. All experiments were carried 3 times independently. $^{*}P < 0.01$ compared with A549-miR-control cells.

of the PIK3CA 3′-UTR were mutated (Fig. 2B). These observations suggest that miR-203 targets PIK3CA 3′-UTR in A549 cells.

To further evaluate the functional relevance of PIK3CA targeting by miR-203, the human PIK3CA coding sequence was inserted into the pTarget vector and PIK3CA expression was regained after transfected with this pTarget-PIK3CA vector. Flow cytometry was used to evaluate the cell cycle of A549 cells co-transfected with either miR-203 mimics or negative control and with either pTarget-PIK3CA or empty pTarget vector. As shown in Fig. 3D that forced expression of PIK3CA rescued S-phase arrest in the presence of miR-203 mimics. Therefore, PIK3CA is a functionally relevant target downstream of miR-203 that modulates the cell cycle in A549 cells.

3.3. Upregulated miR-203 accelerates LPS-induced cell apoptosis

To further investigate the function of miR-203 in LPS-induced apoptosis of A549 cells, we analyzed the cell apoptosis and cell cycle after miR-203 mimic or inhibitor treatment. The treatment of A549 cells with miR-203 mimic alone or with LPS both induced significant increase in cell apoptosis compared with the control group (Fig. 3A). Conversely, miR-203 inhibitor significantly reversed the LPS-induced promotion of cell apoptosis. However, suppression of PIK3CA by siRNA enhanced A549 cell apoptosis, and blocked the inhibitory effect of miR-203 inhibitor on LPS-induced cell apoptosis. It indicated that miR-203 targets PIK3CA in LPS-infected cells.

On the other hand, the proportion of A549 cells in the S-phase after miR-203 mimic or inhibitor treatment was significantly enhanced or diminished, respectively, compared with normal controls ($P < 0.01$). In order to test for a more specific influence on S phase, A549 cells were transfected with miR-203 mimic and at 24 h post-transfection treated with thymidine to arrest cells at the G1/S-boundary. After drug release, cell samples were collected every 2 h over a 6 h period and analyzed cell cycle distribution by

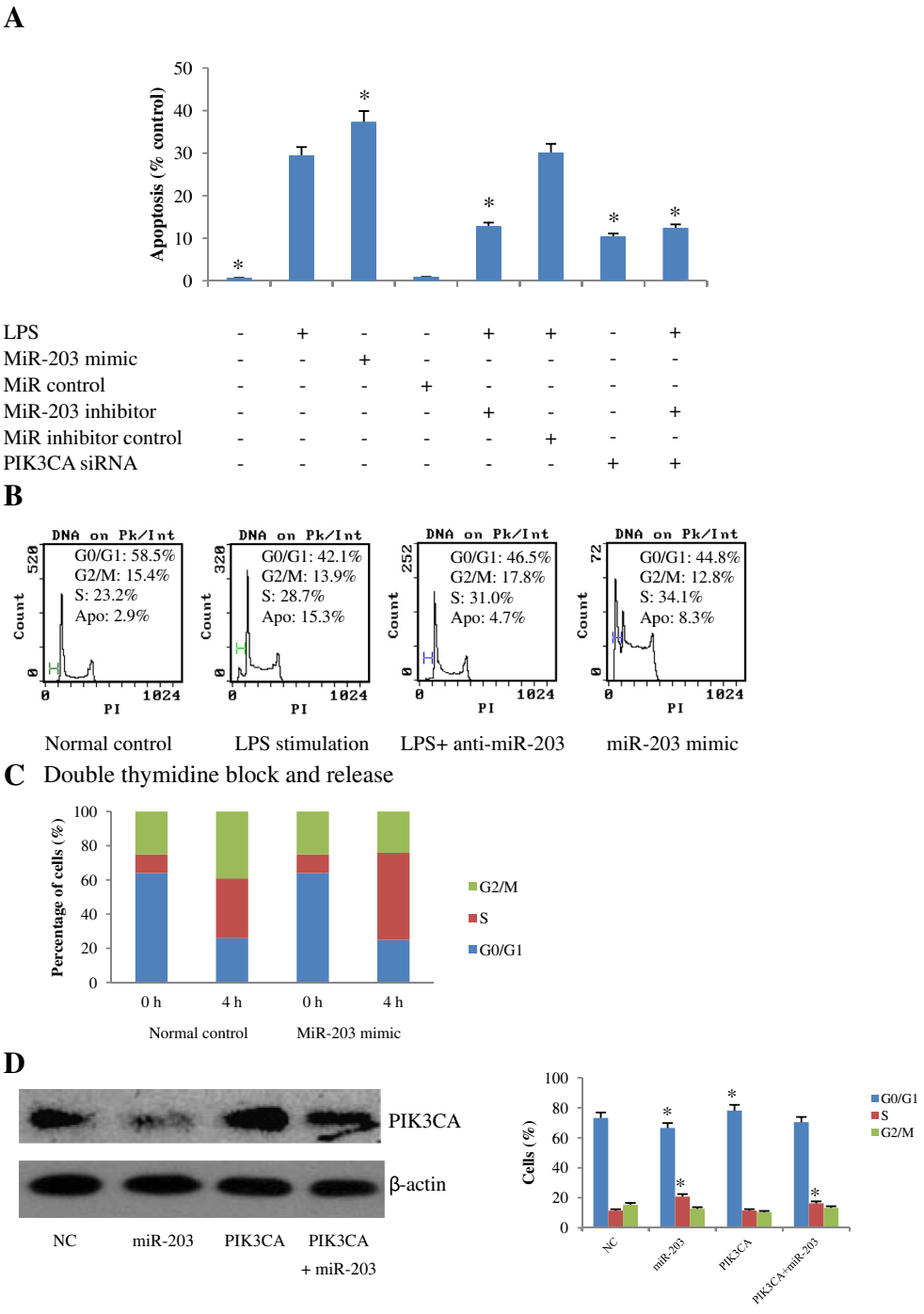

Fig. 3. Induction of miR-203 by LPS contributes to cell apoptosis via inactivation of PI3K/Akt signaling by targeting PIK3CA. (A) Cell apoptosis and (B) cell cycle analysis were performed by FCM. (C) Proportion of cells in S phase at 4 h interval post-release from double thymidine block. (D) Forced expression of PIK3CA rescued miR-203-dependent S-phase arrest. Either miR-203 mimics or NC oligos were co-transfected with pTarget-PIK3CA or empty pTarget vector into A549 cells while western blot analysis was then performed to detect the expression of PIK3CA and GAPDH (Left graph). Forced expression of PIK3CA circumvented the S-phase arrest induced by miR-203 mimics (Right graph). Results were from three independent experiments (*$P < 0.01$).

flow cytometry. As shown in Fig. 3C, upregulation of miR-203 caused a marked delay in the ability of arrested cells to progress beyond the G1/S phase block. Plotting the average S phase values from three experiments showed that the delay was most pronounced within the first two hours post-G1/S release, and thereafter affected progression into G2/M. But there was no difference in S phase progression between control RNAi-transfected cells and untransfected cells (Data not shown). These data indicated that miR-203 could suppress the growth of LPS-stimulated A549 cells by inducing S-phase cell-cycle arrest.

3.4. MiR-203 regulates the PI3K/Akt pathway in LPS-stimulated A549 cells

PIK3CA is an important member of the phosphatidylinositol 3-kinase (PI3K) family. Thus, the expression of key components of the PI3K/Akt pathway was examined in A549 cells with or without miR-203 overexpression. MiR-203 upregulation induced by LPS and treatment with miR-203 mimic also downregulated Akt expression and its activator (p-Akt) in A549 cells, whereas the treatment with miR-203 inhibitor could significantly increase Akt

and p-Akt levels (Fig. 4A). Moreover, the essential regulators of cell apoptosis, namely, Bad, caspase-9, and XIAP, are the downstream targets of the PI3K/Akt pathway. Our results showed that miR-203 overexpression could suppress Akt phosphorylation, subsequently increase apoptotic protein Bad, Bax and caspase-9 levels. Therefore, miR-203 overexpression promotes cell apoptosis.

3.5. MiR-203 antagomir ameliorates LPS-induced ALI in mice

To further confirm the physiological function of miR-203 in LPS-induced apoptosis *in vivo*, we injected miR-203 antagomir into the tail veins every other day after LPS challenge. Compared with the normal control group, the lungs of LPS-challenged mice in model control group showed marked inflammatory alterations characterized by the presence of interstitial edema, hemorrhage, and thickening of the alveolar wall (Fig. 4B). In contrast, histological damage was improved in the ALI mice treated with miR-203 antagomir. Furthermore, compared with the model control, the treatment with miR-203 antagomir significantly reduced the lung index and apoptotic index ($P < 0.01$) as shown in Fig. 4C–E.

4. Discussion

LPS as is a major component of the cell wall of Gram-negative bacteria is an important trigger of ALI [1]. Alveolar epithelial cells

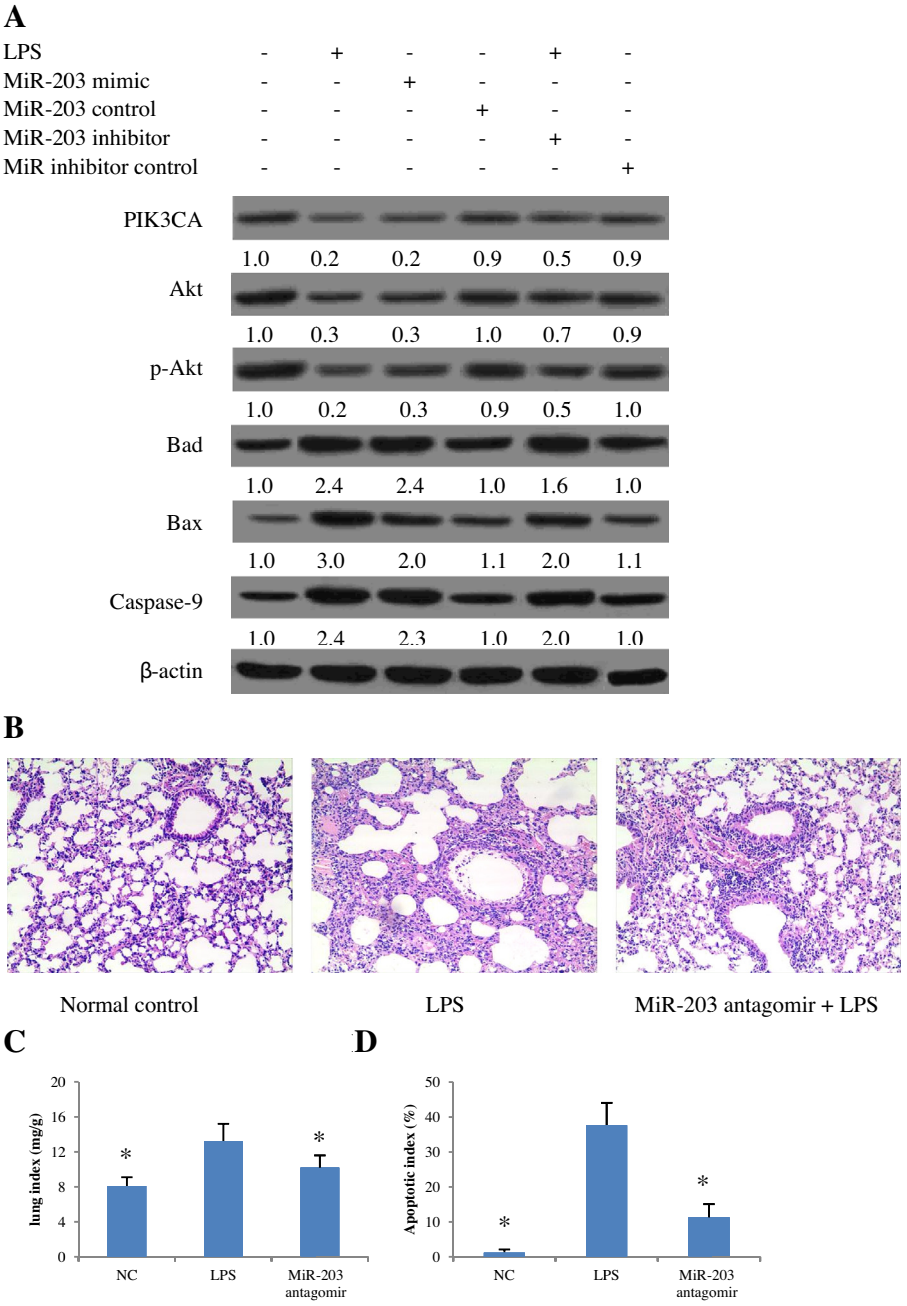

Fig. 4. MiR-203 associates with the cell apoptosis. (A) miR-203 mimic increased the expression of apoptotic proteins (Bad, Bax, and caspase-9) while miR-203 inhibitor reversed these expression in A549 cells. Values below the blots indicated fold changes compared with internal control (β-actin). Suppression of miR-203 ameliorates LPS-induced ALI in mice. Effects of miR-203 antagomir on LPS-induced lung histopathogic changes (B), lung index (C), and apoptotic index (D) Lungs from each experimental group were processed for histological evaluation 24 h after LPS injection. Each bar was represented as mean ± SD ($n = 10$). $^*P < 0.01$ compared with model control group.

(AECs) are often targeted by inflammatory and infectious agents at the epithelial–blood interface, and they participate in the initiation and progression of ALI. Due to the limitations of primary cells, LPS stimulation of A549 cells is a widely used model to simulate the pathogen-associated pattern of ALI *in vitro*.

Apoptosis is closely related to the severity of ALI. It was primarily a host defense mechanism to maintain homeostasis in mammals. However, excessive removal of LPS-stimulated cells by inducing apoptosis results in tissue damage (including multiple organ dysfunctions) and conversely causes effective IAV replication [2]. Post-transcriptional regulation of miRNA-mediated gene expression has an important function in controlling cell apoptosis [15]. Thus, we detected differentially expressed miRNAs at the early and late stages of ALI in murine model to explore new drug targets of the virus propagation through apoptosis regulation.

Given the complex cellular apoptosis pathway activated by LPS challenge, miRNA expression profiling analyzed *in vivo* could simulate more realistic immune responses of the human body when exposed to pathogens. In the present study, we constructed conventional ALI rodent models to replicate the major features of illness in humans. Among the individual miRNAs represented by the microarray analysis, eight apoptosis-related miRNAs were significantly changed in the lung tissue of ALI mice. Moreover, miR-203 expression showed the biggest variation. The upregulation of miR-203 was then confirmed by qPCR. MiR-203 is a typical multifunctional miRNA and has been found to be implicated in viral infections, inflammation, and innate immune response. MiR-203 can be induced by LPS, IFN-β, and TNF-α in macrophages and keratinocytes [16,17]. Overexpression of miR-203 in RAW264.7 cells was correlated with repressions of MyD88, as well as its downstream signaling of NF-κB, TNF-α and IL-6 [18]. Moreover, inhibition of endogenous miR-203 elevated DKK1 expression, which may strengthen Wnt signaling and promote tumor initiation and metastasis *in vivo* [19]. Transfection with miR-203 inhibited proliferation, reduced invasion, induced apoptosis and caused G1 phase cell cycle arrest of Hep-2 cells *in vitro* [20]. Although miR-203 has been shown as a biomarker of clinical importance to inflammation and tumor diagnosis (or therapy), the mechanism that regulates miRNA function and expression has not been completely elucidated. The present study was aimed to determine the miR-203-mediated regulatory mechanism of apoptosis signaling. We observed that miR-203 expression was significantly reduced in the lung tissues of ALI mice. Similar to the results from the lungs, A549 cells exposed to LPS displayed apoptosis and upregulated miR-203 levels.

Using computational target prediction algorithms, PIK3CA was identified as a putative target mRNA of miR-203. A significant decrease in the luciferase reporter translation was detected in the miR-203 mimic-treated cells using a luciferase reporter vector containing PIK3CA 3′ UTR with the putative miR-203 binding site. Moreover, the treatment of cells with miR-203 inhibitor prevented the LPS-induced decrease of PIK3CA expression, whereas a control showed no effect. The results indicated that the inhibition of PIK3CA protein expression by miR-203 could be attributed to the suppression of translational expression induced by LPS.

PIK3CA gene encodes the catalytic subunit of PI3K, and its amplification constitutively activates PI3K/Akt signaling pathway [21]. The activated Akt protein modulates cell proliferation through numerous downstream targets, such as Bad, Bax, mTOR, and caspase-9 [22]. Inhibiting PI3K pathway effectors, such as PIK3CA and Akt, has facilitated the improvement of prognosis and therapeutic outcomes. In the present study, we found that miR-203 overexpression regulated the total and phosphorylated protein levels of Akt and its downstream targets (Bad, Bax, and caspase-9) in A549 cells, indicating that miR-203 may be an important regulator of PI3K/Akt signaling pathway. Furthermore, the LPS-induced cell apoptosis can be blocked by inhibiting miR-203. These results indicated that miR-203 repressed PIK3CA expression, thereby regulating PI3K/Akt pathway. Thus, miR-203 accelerates cell apoptosis.

In summary, the present study demonstrated the mechanism of miR-203 by targeting PIK3CA-accelerated LPS-induced S-phase arrest and apoptosis, which was implemented partially through the repression of the PI3K/Akt pathway. Thus, miR-203 may be a potential apoptotic biomarker and potent therapeutic target for LPS-induced ALI.

Acknowledgments

This work is funded by Zhejiang Academy of Medical Sciences, Zhejiang Provincial Natural Science Foundation (No. Y13H280002), Zhejiang Provincial Science and Technology Foundation (No. 2012F30026) and National Natural Science Foundation of China (No. 81202977).

References

[1] L.B. Ware, M.A. Matthay, The acute respiratory distress syndrome, N. Engl. J. Med. 342 (2000) 1334–1349.
[2] S. Herold, N.M. Gabrielli, I. Vadász, Novel concepts of acute lung injury and alveolar–capillary barrier dysfunction, Am. J. Physiol. Lung Cell. Mol. Physiol. 305 (2013) L665–L681.
[3] R.M. Sweeney, M. Griffiths, D. McAuley, Treatment of acute lung injury: current and emerging pharmacological therapies, Semin. Respir. Crit. Care Med. 34 (2013) 487–498.
[4] W.T. Zhong, Y.C. Wu, X.X. Xie, X. Zhou, M.M. Wei, L.W. Soromou, X.X. Ci, D.C. Wang, Phillyrin attenuates LPS-induced pulmonary inflammation via suppression of MAPK and NF-κB activation in acute lung injury mice, Fitoterapia 90 (2013) 132–139.
[5] X. Chen, X. Yang, T. Liu, M. Guan, X. Feng, W. Dong, X. Chu, J. Liu, X. Tian, X. Ci, H. Li, J. Wei, Y. Deng, X. Deng, G. Chi, Z. Sun, Kaempferol regulates MAPKs and NF-κB signaling pathways to attenuate LPS-induced acute lung injury in mice, Int. Immunopharmacol. 14 (2012) 209–216.
[6] X. Ci, X. Chu, M. Wei, X. Yang, Q. Cai, X. Deng, Different effects of farrerol on an OVA-induced allergic asthma and LPS-induced acute lung injury, PLoS One 7 (2012) e34634.
[7] H.A. Meijer, Y.W. Kong, W.T. Lu, A. Wilczynska, R.V. Spriggs, S.W. Robinson, J.D. Godfrey, A.E. Willis, M. Bushell, Translational repression and eIF4A2 activity are critical for microRNA-mediated gene regulation, Science 340 (2013) 82–85.
[8] J. He, W. Zhang, Q. Zhou, T. Zhao, Y. Song, L. Chai, Y. Li, Low-expression of microRNA-107 inhibits cell apoptosis in glioma by upregulation of SALL4, Int. J. Biochem. Cell Biol. 45 (2013) 1962–1973.
[9] D. Frank, J. Gantenberg, I. Boomgaarden, C. Kuhn, R. Will, K.U. Jarr, M. Eden, K. Kramer, M. Luedde, H. Mairbäurl, H.A. Katus, N. Frey, MicroRNA-20a inhibits stress-induced cardiomyocyte apoptosis involving its novel target Egln3/PHD3, J. Mol. Cell. Cardiol. 52 (2012) 711–717.
[10] J.H. Li, X. Xiao, Y.N. Zhang, Y.M. Wang, L.M. Feng, Y.M. Wu, Y.X. Zhang, MicroRNA miR-886-5p inhibits apoptosis by down-regulating Bax expression in human cervical carcinoma cells, Gynecol. Oncol. 120 (2011) 145–151.
[11] Y.K. Zhang, H. Wang, Y. Leng, Z.L. Li, Y.F. Yang, F.J. Xiao, Q.F. Li, X.Q. Chen, L.S. Wang, Overexpression of microRNA-29b induces apoptosis of multiple myeloma cells through down regulating Mcl-1, Biochem. Biophys. Res. Commun. 414 (2011) 233–239.
[12] J. Wang, B. Yang, L. Han, X. Li, H. Tao, S. Zhang, Y. Hu, Demethylation of miR-9-3 and miR-193a genes suppresses proliferation and promotes apoptosis in non-small cell lung cancer cell lines, Cell Physiol. Biochem. 32 (2013) 1707–1719.
[13] S. Heavey, K.J. O'Byrne, K. Gately, Strategies for co-targeting the PI3K/AKT/mTOR pathway in NSCLC, Cancer Treat. Rev. 40 (2014) 445–456.
[14] S.E. Tang, C.P. Wu, S.Y. Wu, C.K. Peng, W.C. Perng, B.H. Kang, S.J. Chu, K.L. Huang, Stanniocalcin-1 ameliorates lipopolysaccharide-induced pulmonary oxidative stress, inflammation, and apoptosis in mice, Free Radic. Biol. Med. 71 (2014) 321–331.
[15] S. Vineetha, C.C.S. Bhat, S.M. Idicula, MicroRNA–mRNA interaction network using TSK-type recurrent neural fuzzy network, Gene 515 (2013) 385–390.
[16] M.N. Primo, R.O. Bak, B. Schibler, J.G. Mikkelsen, Regulation of pro-inflammatory cytokines TNFα and IL24 by microRNA-203 in primary keratinocytes, Cytokine 60 (2012) 741–748.
[17] E. Sonkoly, M. Ståhle, A. Pivarcsi, MicroRNAs and immunity: novel players in the regulation of normal immune function and inflammation, Semin. Cancer Biol. 18 (2008) 131–140.
[18] J. Wei, X. Huang, Z. Zhang, W. Jia, Z. Zhao, Y. Zhang, X. Liu, G. Xu, MyD88 as a target of microRNA-203 in regulation of lipopolysaccharide or Bacille Calmette-Guerin induced inflammatory response of macrophage RAW264.7 cells, Mol. Immunol. 55 (2013) 303–309.

[19] J.H. Taube, G.G. Malouf, E. Lu, N. Sphyris, V. Vijay, P.P. Ramachandran, K.R. Ueno, S. Gaur, M.S. Nicoloso, S. Rossi, J.I. Herschkowitz, J.M. Rosen, J.P. Issa, G.A. Calin, J.T. Chang, S.A. Mani, Epigenetic silencing of microRNA-203 is required for EMT and cancer stem cell properties, Sci. Rep. 3 (2013) 2687.
[20] L. Tian, M. Li, J. Ge, Y. Guo, Y. Sun, M. Liu, H. Xiao, MiR-203 is downregulated in laryngeal squamous cell carcinoma and can suppress proliferation and induce apoptosis of tumours, Tumour Biol. 35 (2014) 5953–5963.
[21] F. Janku, D.S. Hong, S. Fu, S.A. Piha-Paul, A. Naing, G.S. Falchook, A.M. Tsimberidou, V.M. Stepanek, S.L. Moulder, J.J. Lee, R. Luthra, R.G. Zinner, R.R. Broaddus, J.J. Wheler, R. Kurzrock, Assessing PIK3CA and PTEN in early-phase trials with PI3K/AKT/mTOR inhibitors, Cell Rep. 6 (2014) 377–387.
[22] J.A. Fresno Vara, E. Casado, J. de Castro, P. Cejas, C. Belda-Iniesta, M. González-Barón, PI3K/Akt signalling pathway and cancer, Cancer Treat. Rev. 30 (2004) 193–204.